

## RESEARCH ARTICLE

# Stellate and pyramidal neurons in goldfish telencephalon respond differently to anoxia and GABA receptor inhibition

Nariman Hossein-Javaheri<sup>1</sup>, Michael P. Wilkie<sup>2</sup>, Wudu E. Lado<sup>3</sup> and Leslie T. Buck<sup>1,\*</sup>

## ABSTRACT

With oxygen deprivation, the mammalian brain undergoes hyperactivity and neuronal death while this does not occur in the anoxia-tolerant goldfish (*Carassius auratus*). Anoxic survival of the goldfish may rely on neuromodulatory mechanisms to suppress neuronal hyper-excitability. As  $\gamma$ -aminobutyric acid (GABA) is the major inhibitory neurotransmitter in the brain, we decided to investigate its potential role in suppressing the electrical activity of goldfish telencephalic neurons. Utilizing whole-cell patch-clamp recording, we recorded the electrical activities of both excitatory (pyramidal) and inhibitory (stellate) neurons. With anoxia, membrane potential ( $V_m$ ) depolarized in both cell types from  $-72.2$  mV to  $-57.7$  mV and from  $-64.5$  mV to  $-46.8$  mV in pyramidal and stellate neurons, respectively. While pyramidal cells remained mostly quiescent, action potential frequency ( $AP_f$ ) of the stellate neurons increased 68-fold. Furthermore, the GABA<sub>A</sub> receptor reversal potential ( $E_{GABA}$ ) was determined using the gramicidin perforated-patch-clamp method and found to be depolarizing in pyramidal ( $-53.8$  mV) and stellate neurons ( $-42.1$  mV). Although GABA was depolarizing, pyramidal neurons remained quiescent as  $E_{GABA}$  was below the action potential threshold ( $-36$  mV pyramidal and  $-38$  mV stellate neurons). Inhibition of GABA<sub>A</sub> receptors with gabazine reversed the anoxia-mediated response. While GABA<sub>B</sub> receptor inhibition alone did not affect the anoxic response, co-antagonism of GABA<sub>A</sub> and GABA<sub>B</sub> receptors (gabazine and CGP-55848) led to the generation of seizure-like activities in both neuron types. We conclude that with anoxia,  $V_m$  depolarizes towards  $E_{GABA}$  which increases  $AP_f$  in stellate neurons and decreases  $AP_f$  in pyramidal neurons, and that GABA plays an important role in the anoxia tolerance of goldfish brain.

**KEY WORDS:** Action potential, Spike frequency, Whole-cell conductance, Membrane potential, Action potential frequency,  $E_{GABA}$

## INTRODUCTION

During periods of oxygen deprivation, ATP synthesis in the anoxia-intolerant brain (mammals) halts and compromises the ability of the  $Na^+/K^+$ -ATPase pump to maintain neuronal ion gradients, leading to membrane depolarization (Hansen, 1985). The release of excitatory neurotransmitters (glutamate, aspartate) follows, leading to activation of  $\alpha$ -amino-3-hydroxy-5-methyl-4-isoxazolepropionic


acid (AMPA) and *N*-methyl-D-aspartate (NMDA) receptors (Sattler and Tymianski, 2000). Subsequent calcium ( $Ca^{2+}$ ) influx through NMDA receptors causes further depolarization of membrane potential ( $V_m$ ), and activates intracellular  $Ca^{2+}$ -dependent signaling cascades, which leads to neuronal hyper-excitability and, eventually, excitotoxic cell death (Sattler and Tymianski, 2000). As anoxia eliminates oxidative phosphorylation, the glycolytic pathway becomes the major source of ATP produced by the brain, generating less than 1/10th of the ATP produced under normoxic conditions (Hochachka, 1986). The ATP shortfall is particularly problematic for neurons, as action potential propagation, consequent activation of output synapses and maintenance of neuronal ion gradients are metabolically expensive events, consuming approximately 60% of the total brain ATP turnover (Erecińska and Silver, 1994). Anoxia-tolerant organisms, such as the western painted turtle (*Chrysemys picta*), avoid anoxia-mediated cellular injury by not only reducing ATP synthesis by over 90% (Bickler and Buck, 2007) but also reducing ATP demand; indeed, in the case of turtle cortical pyramidal neurons, an anoxia-mediated 60–70% reduction in action potential frequency ( $AP_f$ ) has been reported (Pamenter et al., 2011).

There are three hypotheses that encompass the events that lead to a large decrease in metabolic rate such as that exhibited by anoxia-tolerant species; these are the metabolic arrest (MA), channel arrest (CA) and spike arrest (SA) hypotheses (Hochachka, 1986; Lutz, 1992; Buck and Hochachka, 1993). The MA hypothesis generally describes events leading to a reduction in ATP supply, while the CA hypothesis is specific to a reduction in ion channel conductance leading to a reduction in ATP demand. The SA hypothesis is specific to neurons or excitable tissues and entails a reduction in  $AP_f$  that leads to a reduction in ATP demand and therefore a reduction in ATP supply (Hochachka et al., 1996). Neurons function within an integrated network; therefore, mechanisms regulating metabolic rate are also likely to occur at the network level. Specifically, with the onset of anoxia, some neurons may be activated in order to inhibit other neurons. We found evidence of this in anoxia-tolerant turtle cortical neurons, where glutamatergic pyramidal neurons undergo spike arrest as a result of an increase in inhibitory  $\gamma$ -aminobutyric acid type A (GABA<sub>A</sub>) receptor currents (Pamenter et al., 2011). However, we have not recorded directly from the likely source of the increased GABA levels – stellate interneurons.

Stellate neurons are smaller than pyramidal neurons and are more difficult to patch clamp in the turtle cortex (Connors and Kriegstein, 1986); therefore, our present goal was to develop a brain slice model in which stellate neurons could be reliably patched to obtain recordings during a normoxic to anoxic transition. As the reversal potential ( $E_{GABA}$ ) for the GABA<sub>A</sub> receptor is depolarized relative to  $V_m$  in the turtle pyramidal neurons, we also set out to determine  $E_{GABA}$  in both goldfish stellate and pyramidal neurons. We hypothesized that, with the onset of anoxia, stellate neuron  $V_m$  will depolarize towards  $E_{GABA}$ , and  $AP_f$  will increase. Furthermore, we hypothesized that pyramidal

<sup>1</sup>Department of Cell and Systems Biology, University of Toronto, 25 Harbord St, Toronto, ON, Canada M5S 3G5. <sup>2</sup>Department of Biology, Wilfrid Laurier University, 75 University Avenue West, Waterloo, ON, Canada N2L 3C5. <sup>3</sup>Department of Neurobiology, University of Alabama at Birmingham, 1825 University Blvd, Birmingham, AL 35294-2182, USA.

\*Author for correspondence (les.buck@utoronto.ca)

 L.T.B., 0000-0002-2637-7821

**List of abbreviations**

aCSF	artificial cerebrospinal fluid
AMPA	$\alpha$ -amino-3-hydroxy-5-methyl-4-isoxazolepropionic acid
AMPK	AMP-dependent protein kinase
AP <sub>f</sub>	action potential frequency
AP <sub>th</sub>	action potential threshold
APV	(2R)-amino-5-phosphonovaleric acid
BIC	bicuculline
CGP	CGP-55848
CNQX	6-cyano-7-nitroquinoxaline-2,3-dione
$E_{\text{GABA}}$	GABA reversal potential
EPSP	excitatory post-synaptic potential
GABA	$\gamma$ -aminobutyric acid
GIRK	G-protein coupled inwardly rectifying potassium channel
$G_w$	whole-cell conductance
GZ	gabazine (SR95531)
$I/V$	current–voltage
NMDA	N-methyl-D-aspartate
TTX	tetrodotoxin
$V_m$	membrane potential

neuron  $V_m$  will depolarize towards  $E_{\text{GABA}}$ , and whole-cell conductance will increase but AP<sub>f</sub> will decrease.

**MATERIALS AND METHODS****Animals**

This study was approved by the University of Toronto Animal Care Committee and conforms to the relevant guidelines issued by the Canadian Council of Animal Care regarding the care and use of experimental animals. Common goldfish, *Carassius auratus* (Linnaeus 1758), weighing 50–100 g were purchased from a commercial supplier (AQUALITY Tropical Fish Wholesale, Mississauga, ON, Canada) and held in flowing dechlorinated City of Toronto tap water at 18°C at the University of Toronto.

**Golgi staining**

Whole goldfish brain was removed from the cranium following decapitation and the entire brain underwent Golgi staining. This technique reveals fine structures of neurons, glia and their processes, allowing a better understanding of cellular morphology along with their orientation and location in cortical slices (Melendez-Ferro et al., 2009). Tissue was fixed in 10% formalin for 2 days followed by fixation in 3% K<sub>2</sub>Cr<sub>2</sub>O<sub>7</sub> for 1 day and 2% AgNO<sub>3</sub> for another 2 days (Olude et al., 2015). The telencephalon was separated from the rest of the brain and sliced into 100  $\mu\text{m}$ -thick axial slices using a Leica VT1200S vibratome (Leica, Richmond Hill, ON, Canada). Slices were collected using a soft brush, placed on a microscope slide, cover-slipped and stored at 4°C.

**Whole-cell electrophysiology**

Telencephalon dissection, tissue preparation and whole-cell patch-clamp recording methods are described elsewhere (Wilkie et al., 2008). In short, the whole brain of the goldfish was removed from the cranium after decapitation and was placed in oxygenated ice-cold 4°C artificial cerebrospinal fluid (aCSF) containing (in mmol l<sup>-1</sup>): 20 NaHCO<sub>3</sub>, 118 NaCl, 1.2 MgCl<sub>2</sub>·6H<sub>2</sub>O, 1.2 KH<sub>2</sub>PO<sub>4</sub>, 1.9 KCl, 10 Hepes-Na, 10 D-glucose and 2.4 CaCl<sub>2</sub> (pH 7.6, adjusted with HCl); osmolarity 285–290 mOsm. Both lobes of telencephalon were then dissected from the rest of the brain while in the chilled aCSF. Each telencephalon lobe was glued to a sectioning plate on a vibratome slicing chamber using cyanoacrylate glue (Krazy Glue) and was filled with 4°C aCSF. Isolated goldfish telencephalon was cut into 300  $\mu\text{m}$  slices using a

VT1200S vibratome. Slices were lifted out of the chamber and were stored in vials of oxygenated aCSF for no longer than 48 h. Slices remained physiologically viable up to 48 h in the preparation (Wilkie et al., 2008). During each experiment, individual telencephalon slices were perfused with either oxygenated (99% O<sub>2</sub>, 1% CO<sub>2</sub>) or anoxic (99% N<sub>2</sub>, 1% CO<sub>2</sub>) aCSF (composition described above), and whole-cell recordings were performed using the voltage-clamp method with 9–11 M $\Omega$  borosilicate glass pipette electrodes (Harvard Apparatus Ltd, Holliston, MA, USA) containing the following (in mmol l<sup>-1</sup>): 120 potassium gluconate, 10 KCl, 15 sucrose, 2 Na<sub>2</sub>ATP, 0.44 CaCl<sub>2</sub>, 1 EGTA and 10 Hepes-Na (pH 7.6 adjusted with KOH); osmolarity 285–290 mOsm. The electrode was connected to a CV-4 headstage (gain: 1/100 U, Axon Instruments, Sunnyvale, CA, USA) and an Axopatch 1D patch-clamp amplifier (Axon Instruments). A whole-cell patch configuration was established by voltage clamping the recording potential to –60 mV and applying negative pressure after a 1–20 G $\Omega$  seal was established. All seals were obtained using the blind-patch technique (Blanton et al., 1989). Whole-cell capacitance was compensated, typical whole-cell access resistance was 30–40 M $\Omega$  and series resistance was not greater than 50 M $\Omega$ . Access resistance was monitored periodically and data were discarded if it changed by 10–15 M $\Omega$ . Electrophysiological recordings were performed on pyramidal neurons and stellate neurons in goldfish telencephalon. The cerebral cortex of fish, amphibians and reptiles is characterized by three layers, in which the pyramidal neurons are excitatory glutamatergic cells and the stellate neurons are primarily GABAergic and inhibitory, providing feed-forward and feedback inhibition to pyramidal cells (Shepherd, 2011; Larkum et al., 2008). Electrophysiologically, the two cell types were differentiated in goldfish telencephalon by their responses to somatic current injections which produce trains of action potentials. If accommodation occurred quickly, the cell was distinguished as a pyramidal neuron and if no accommodation was observed, the cell was differentiated as a stellate neuron. Further, neural morphology was determined by filling the microelectrode solution with 5% Lucifer Yellow in 2 mol l<sup>-1</sup> LiCl. Lucifer Yellow was ejected by steady hyperpolarizing current for 5 min after completion of the experiment (Connors and Kriegsten, 1986; Shin and Buck, 2003). Spontaneous electrical activity was recorded for approximately 1 h (5–10 min normoxia, 30 min anoxia, 20 min recovery) from pyramidal and stellate neurons. Action potential threshold (AP<sub>th</sub>) was determined by injecting current in a ramp manner in 1 nA steps until an AP was elicited. Whole-cell conductance ( $G_w$ ) was measured by clamping neurons at voltage steps from –90 to –30 mV in 10 mV increments, lasting 200 ms each. Current amplitudes were measured between 135 and 145 ms and a slope conductance according to the current–voltage ( $I/V$ ) relationship was determined (Pamenter et al., 2011).

**Perforated-patch electrophysiology**

We utilized the gramicidin perforated-patch technique to determine  $E_{\text{GABA}}$  without perturbing neural Cl<sup>-</sup> gradients. Micropipette tips were front-filled with electrode recording solution by applying suction to the back of the pipette for 30 s, then back-filled with a solution of 13  $\mu\text{g ml}^{-1}$  gramicidin in DMSO dissolved in electrode solution.  $G_w$  recordings and  $I/V$  relationships were analyzed by taking the linear regression of each line before and during 2 mmol l<sup>-1</sup> GABA application.  $E_{\text{GABA}}$  was estimated by measuring the voltage at which the  $I/V$  relationships before and during GABA application intersected (Watanabe et al., 2009). Using the Nernst equation and the known extracellular [Cl<sup>-</sup>], we estimated the intracellular [Cl<sup>-</sup>] from  $E_{\text{GABA}}$ .  $E_{\text{GABA}}$  was calculated by deducting conductance values pre- and post-GABA application, and plotting the results on a  $I/V$  curve.

## Pharmacology

Goldfish telencephalon slices were perfused with pharmacological modifiers as specified in the Results through a fast-step perfusion system (VC-6 perfusion valve controller and SF-77B fast-step perfusion system; Warner Instruments, Hamden, CT, USA). Possible involvement of the GABAergic system in the anoxic response was investigated by application of GABA<sub>A</sub> and GABA<sub>B</sub> receptor antagonists, 25  $\mu\text{mol l}^{-1}$  SR95531 gabazine (GZ), 5  $\mu\text{mol l}^{-1}$  CGP-55848 (CGP) and 100  $\mu\text{mol l}^{-1}$  bicuculline (BIC) during anoxia. Changes in  $V_m$  and  $\text{AP}_f$  post-drug application were compared. AMPA and NMDA receptors were blocked using 25  $\mu\text{mol l}^{-1}$  of 6-cyano-7-nitroquinoxaline-2,3-dione (CNQX) and 25  $\mu\text{mol l}^{-1}$  (2R)-amino-5-phosphonovaleric acid (APV), respectively. Voltage-gated sodium channels were blocked with 1  $\mu\text{mol l}^{-1}$  tetrodotoxin (TTX).  $E_{\text{GABA}}$  was obtained by perfusing cortical slices with 2  $\text{mmol l}^{-1}$  GABA. All chemicals were obtained from Sigma-Aldrich Canada Ltd (Oakville, ON, Canada) except CGP and TTX, which were obtained from Tocris Cookson (Bristol, UK).

## Statistics

Electrophysiological data were analyzed using SigmaPlot (version 11.0; Systat Software, Inc., San Jose, CA, USA). All data were tested for normality and equal variance and an analysis of

variance (repeated measure ANOVA) was used for between-group comparisons where appropriate. *Post hoc* analyses consisted of Holm–Sidak or Tukey’s test. Data are expressed as means  $\pm$  s.e.m.;  $n$  values represent a recording from a single cell from a single telencephalic slice of a single goldfish.  $P < 0.05$  was considered statistically significant.

## RESULTS

### Goldfish telencephalic neurons are divided into distinct medially and laterally localized regions

Golgi staining and fluorescence imaging revealed that goldfish telencephalon neurons were located in two distinct regions. The first neural cell population was located at the lateral regions and cells were spread into distinct layers (Fig. 1A). For simplicity, we divided the cells into three types. Type one cells had a triangular shaped soma with dendritic fields extending away from the cell body in both apical and basal directions (Fig. 1B,D). Their dendritic extensions were large with medial projections towards the center of the slice. With application of a suprathreshold current pulse, these neurons showed rapid adaptation and fired distinct action potentials followed by hyperpolarization (Fig. 1F). Cells with these characteristics were identified in painted turtle cortex as pyramidal neurons (Connors and Kriegsten, 1986). Type two cells had a small ( $\sim 25 \mu\text{m}$ ) and circular soma with bi-lateral projections extending

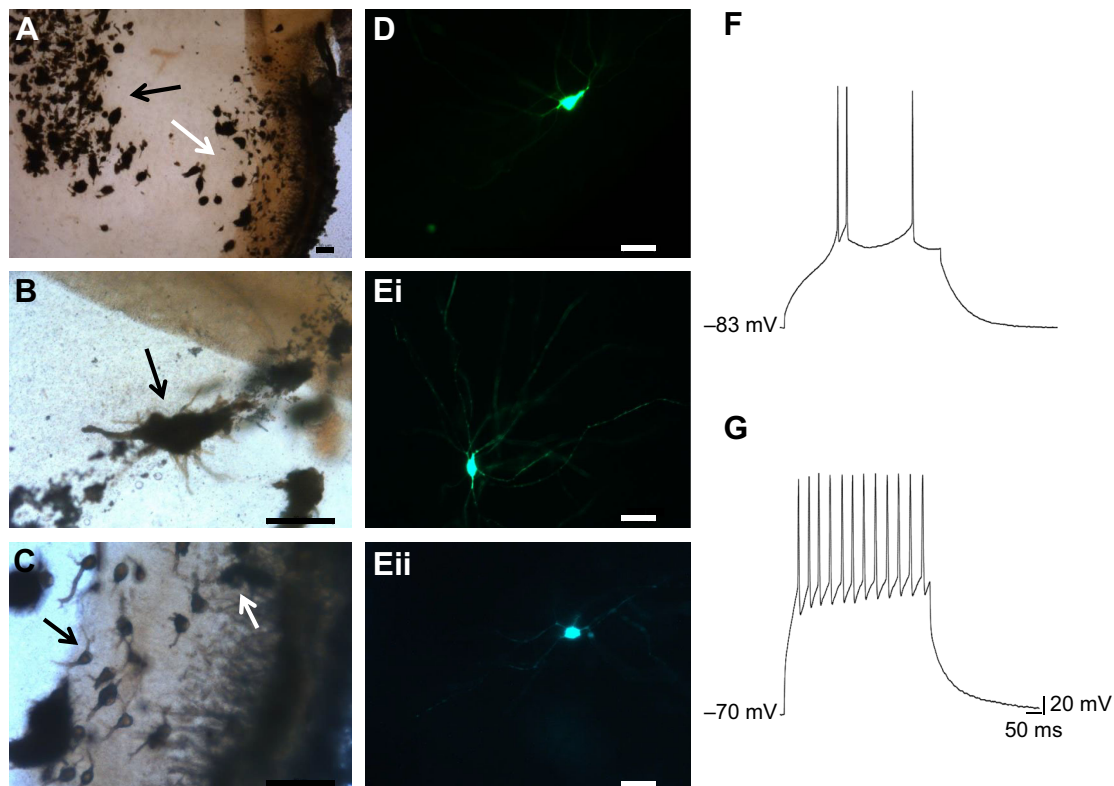


**Fig. 1. Goldfish telencephalic neurons.** (A) An example of a goldfish telencephalon slice following Golgi staining, enlarged 10 $\times$ . Cells were concentrated at two distinct medial and lateral regions. The two populations were clearly separated by white matter and connective tissue. *Area dorsalis telencephali pars centralis*, indicated by the black arrow, was the medial region of the slice, which contained a large population of pyramidal neurons. The lateral regions, indicated by white arrow, contained both small, localized and large stellate cells with medial projections. (B) A pyramidal cell magnified 40 $\times$ . These cells showed two apical and basal outward projections from their triangular shaped soma. (C) A group of stellate cells with circular shaped somas were largely concentrated closer to the edges and appeared to be divided into layers. (D) A pyramidal neuron filled with Lucifer Yellow and imaged immediately after whole-cell recording. These cells expressed the same morphology observed with Golgi staining. (Ei) A stellate cell with a large dendritic tree and bi-lateral projections. (Eii) Small stellate neurons that were more concentrated at the lateral region. (F,G) Action potential properties of pyramidal (F) and stellate (G) neurons recorded under current clamp. The pyramidal cells are rapidly adapting neurons while stellate neurons are slowly adapting and can generate action potentials rapidly in response to injected current. The scale bars represent 50  $\mu\text{m}$ .



away from the cell body (Fig. 1C). It appeared that these cells were more localized and had little branching on their dendritic tree (Fig. 1Eii). Type three cells had a more oval-shaped cell body, which was larger than type two cells ( $\sim 50\ \mu\text{m}$ ) (Fig. 1Ei). Similar to pyramidal neurons, they sent their projections medially and had large dendritic fields. Physiologically, both type two and type three cells showed little or no spike frequency accommodation in response to suprathreshold current. Action potentials were generated continuously and had equal amplitude (Fig. 1G). This physiological morphology has been associated with stellate neurons (Connors and Kriegstein, 1986).

The second population was part of the *area dorsalis telencephali pars centralis* located at the center of the slice and was isolated from the lateral region (Peter and Gill, 1975). The *area dorsalis telencephali pars centralis* contained both pyramidal and type three stellate neurons; however, no type two stellate neurons were observed. Perhaps because of their small size, type two stellate neurons were encountered only twice. Hence, data collected from these cells were excluded from the data set. Both pyramidal and stellate cells had large dendritic trees and were highly interconnected. In this experiment, the term ‘stellate neurons’ refers to the type three stellate cells.

### Pyramidal and stellate neurons respond differently to anoxia

Pyramidal neurons are the primary excitatory neurons in the turtle cortex and are the major consumers of ATP (Howarth et al., 2010). A reduction in excitability of these neurons is crucial to tolerance of anoxia and ischemia, and energy conservation (Pamenter et al., 2011; Hogg et al., 2015). Inhibition is not independent from the rest of the cortex and if GABAergic stimulation is responsible for suppression of neuronal excitability, the inhibitory stellate cells should show greater excitation with anoxia. Under passive recording conditions ( $I=0$ ), it was observed that pyramidal neurons were mostly quiescent and  $V_m$  was maintained at  $-72.18 \pm 2.3\ \text{mV}$  during normoxia.  $V_m$  depolarized to  $-57.7 \pm 1.6\ \text{mV}$  after 30 min of anoxia ( $P=0.01$ ,  $n=14$ ) and repolarized to  $-64.22 \pm 2.6\ \text{mV}$  after 20 min of normoxic recovery ( $P=0.08$ ,  $n=14$ ). Despite  $V_m$  depolarization, these cells did not generate an action potential (Fig. 2A,E,F). However, a small population of pyramidal neurons were more depolarized and active during normoxia ( $V_m = -60.5 \pm 1.6\ \text{mV}$ ,  $\text{AP}_f = 0.51 \pm 0.03\ \text{Hz}$ ). In these cells, anoxic treatment caused a depolarization of  $V_m$  to  $-53 \pm 1.08\ \text{mV}$  ( $P=0.04$ ,  $n=4$ ) and  $\text{AP}_f$  decreased to  $0.1 \pm 0.06\ \text{Hz}$  ( $P<0.001$ ,  $n=4$ ). With normoxic recovery,  $V_m$  hyperpolarized to  $-55 \pm 2.6\ \text{mV}$ ; however, this was not significantly different from anoxic  $V_m$ ;  $\text{AP}_f$  increased to  $0.24 \pm 0.1\ \text{Hz}$  ( $P=0.003$  from anoxia to recovery,  $n=4$ ) (Fig. 2D,G,H). Similar to findings in pyramidal neurons,  $V_m$  depolarized from  $-64.54 \pm 1.05\ \text{mV}$  to  $-46.86 \pm 1.2\ \text{mV}$  and repolarized to  $-53 \pm 2.65\ \text{mV}$  in stellate neurons during a normoxic to anoxic transition and recovery ( $P=0.02$  for normoxia to anoxia and  $P=0.03$  for anoxia to recovery,  $n=11$ ). Unlike pyramidal neurons, stellate neurons generated action potentials with anoxia and  $\text{AP}_f$  increased from  $0.03 \pm 0.009\ \text{Hz}$  to  $2.04 \pm 0.12\ \text{Hz}$  ( $P<0.001$ ,  $n=11$ ).  $\text{AP}_f$  was reduced to  $0.13 \pm 0.03\ \text{Hz}$  with normoxic recovery ( $P<0.001$ ,  $n=11$ ) (Fig. 2B,E,F). Application of AMPA and NMDA receptor antagonists ( $25\ \mu\text{mol l}^{-1}$  CNQX and  $25\ \mu\text{mol l}^{-1}$  APV, respectively) did not suppress action potentials; however,  $1\ \mu\text{mol l}^{-1}$  TTX abolished them (data not shown). Furthermore, both pyramidal and stellate neurons showed an  $\sim 60\%$  increase in  $G_w$  with anoxia. These changes were from  $1.75 \pm 0.34\ \text{nS}$  to  $2.83 \pm 0.17\ \text{nS}$  in pyramidal neurons ( $P=0.04$ ,  $n=7$ ) and  $1.27 \pm 0.15\ \text{nS}$  to  $2.01 \pm 0.16\ \text{nS}$  in stellate cells ( $P=0.07$ ,  $n=8$ ) (Fig. 2G).

### $V_m$ shifts towards $E_{\text{GABA}}$ with anoxia

Activation of  $\text{GABA}_A$  receptors leads to a  $\text{Cl}^-$  flux in the direction of the reversal potential ( $E_{\text{Cl}}$ ) (Blaesse et al., 2009). As  $\text{GABA}_A$  receptors are predominantly permeable to  $\text{Cl}^-$ ,  $E_{\text{GABA}}$  and  $E_{\text{Cl}}$  should be similar (Errington et al., 2014). We measured  $E_{\text{GABA}}$  in goldfish telencephalic neurons to better understand the relationship between  $V_m$  and  $E_{\text{GABA}}$ . In order not to perturb neuronal  $\text{Cl}^-$  gradients, we used the gramicidin perforated-patch technique to determine  $E_{\text{GABA}}$ . Addition of  $2\ \text{mmol l}^{-1}$  GABA during normoxia increased  $V_m$  in telencephalic neurons by  $20 \pm 2.6\ \text{mV}$  ( $n=8$  for pyramidal neurons and  $n=8$  for stellate neurons,  $P<0.001$ ), which returned to baseline approximately 10 min post-GABA application (Fig. 3A). In pyramidal neurons, stepwise current injection generated action potentials in the absence of GABA but not in the presence of GABA (Fig. 3B). Similarly, stellate neurons showed suppressed activity with GABA application; however, with increased current injection, these neurons were capable of generating action potentials (Fig. 3C). Furthermore,  $G_w$  was recorded before and after GABA application and a  $I/V$  relationship was constructed. GABA increased  $G_w$  and the intersection between the two  $I/V$  curves was taken as  $E_{\text{GABA}}$  (Fig. 3D).  $E_{\text{GABA}}$  was more depolarized in stellate neurons than in pyramidal cells:  $-42.1 \pm 2.3$  and  $-53.80 \pm 2.63\ \text{mV}$ , respectively. By obtaining the  $E_{\text{GABA}}$  values and utilizing the Nernst equation, we were able to calculate intracellular  $[\text{Cl}^-]$ , which was  $\sim 15.1$  and  $\sim 24\ \text{mmol l}^{-1}$  in pyramidal and stellate neurons, respectively. As demonstrated previously,  $G_w$  increased with anoxia from  $3.96 \pm 0.95\ \text{nS}$  to  $6.84 \pm 0.61\ \text{nS}$  ( $P<0.001$ ,  $n=5$ ). Addition of GABA appeared to increase  $G_w$  during normoxia; however, this increase was not significant ( $G_w = 5.49 \pm 0.86\ \text{nS}$ ,  $P=0.3$ ,  $n=5$ ). With anoxia,  $G_w$  increased to  $8.49 \pm 0.2\ \text{nS}$ , which was significantly different from anoxia without GABA ( $P=0.02$ ,  $n=5$ ) and from normoxia with GABA ( $P<0.001$ ,  $n=5$ ) (Fig. 3E).

### Anoxic $V_m$ depolarization is reversed by inhibition of $\text{GABA}_A$ and $\text{GABA}_B$ receptors

In order to investigate the possible role of GABA in the defense against anoxia-mediated damage in goldfish telencephalic neurons, we blocked  $\text{GABA}_A$  and  $\text{GABA}_B$  receptors under anoxic conditions. During anoxia, pyramidal neuron  $V_m$  hyperpolarized with application of the  $\text{GABA}_A$  receptor inhibitor GZ ( $25\ \mu\text{mol l}^{-1}$ ) from  $-56.54 \pm 1.7\ \text{mV}$  to  $-64.77 \pm 1.9\ \text{mV}$  and depolarized back to  $-55.15 \pm 1.36\ \text{mV}$  with normoxic recovery ( $P<0.001$ ,  $n=6$ ) (Fig. 4A,D). In anoxic stellate neurons, GZ also hyperpolarized  $V_m$  from  $-46.8 \pm 2.1\ \text{mV}$  to  $-58.54 \pm 2.1\ \text{mV}$  ( $P<0.001$ ,  $n=5$ ) (Fig. 4B,D) and  $\text{AP}_f$  decreased from  $2.04 \pm 0.12\ \text{Hz}$  to  $0.155 \pm 0.01\ \text{Hz}$  ( $P<0.001$ ,  $n=5$ ) (Fig. 4E). These changes were reversed with the termination of GZ application. The  $\text{GABA}_A$  receptor inhibitor BIC also hyperpolarized  $V_m$  to  $-68.82 \pm 1.7\ \text{mV}$  and  $-56.8 \pm 1.97\ \text{mV}$  in pyramidal and stellate neurons, respectively ( $n=3$ ,  $P<0.001$ ; data not shown). No significant difference was observed between BIC and GZ in reversal of the anoxic response. Even though the  $\text{GABA}_B$  receptor antagonist CGP alone did not change  $V_m$  or  $\text{AP}_f$  in either cell type ( $V_m = -53.97 \pm 2.24\ \text{mV}$  for pyramidal and  $V_m = -47.74 \pm 2.83\ \text{mV}$ ,  $n=4$ ), co-antagonism of  $\text{GABA}_A$  and  $\text{GABA}_B$  receptors with GZ plus CGP significantly influenced neuronal excitability (Fig. 4E). GZ+CGP initially hyperpolarized  $V_m$  similar to what was observed with GZ perfusion. However, shortly after,  $V_m$  depolarized significantly ( $V_m = -36.58 \pm 1.62$ ,  $P<0.001$ ,  $n=4$ , and  $-34.25 \pm 5.9\ \text{mV}$ ,  $P<0.001$ ,  $n=5$  for pyramidal and stellate neurons, respectively) and generated sudden, seizure-like action potentials (Fig. 4C,D). Furthermore,  $\text{AP}_f$  increased in pyramidal neurons from

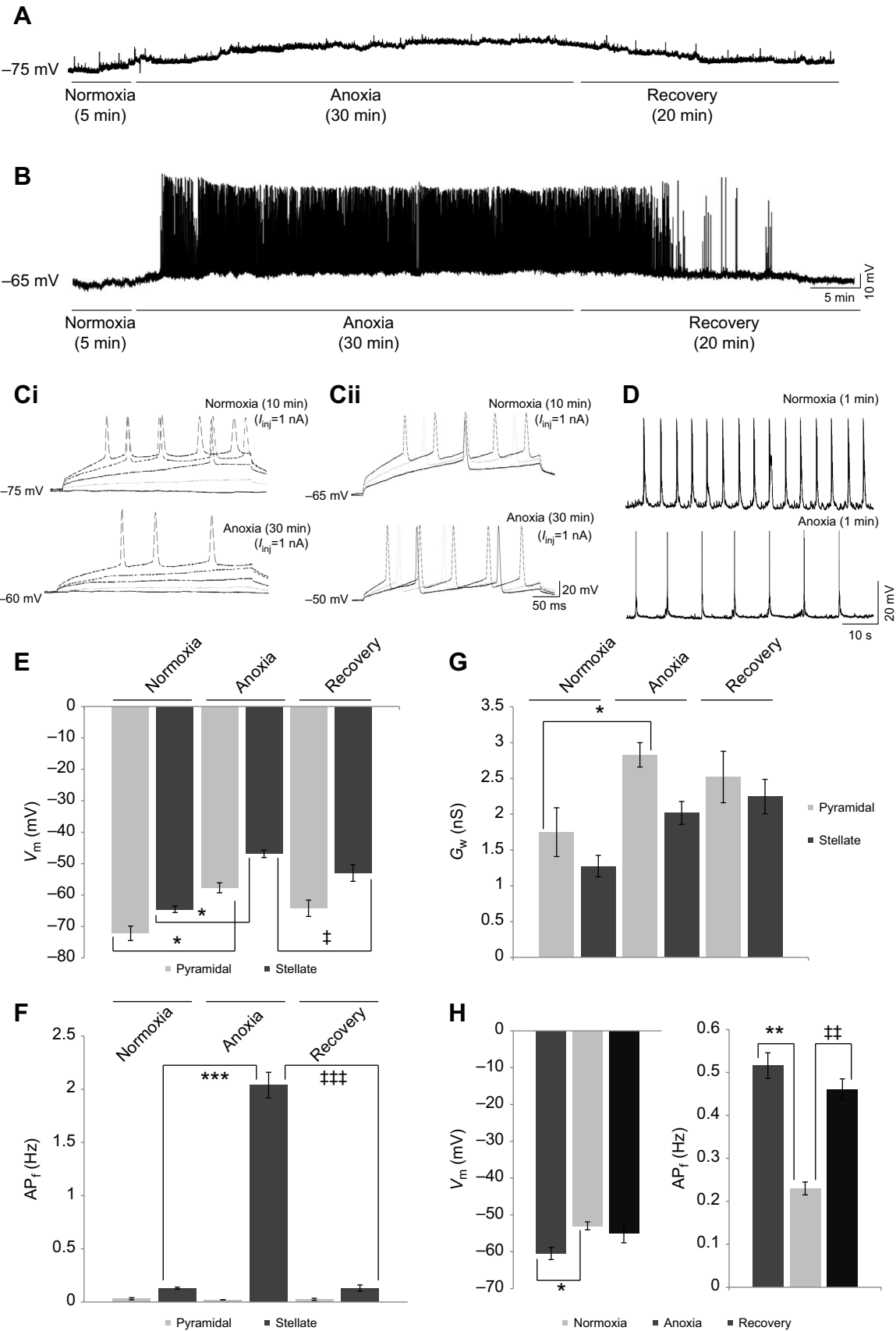


Fig. 2. See next page for legend.

**Fig. 2. Basic electrophysiological properties of pyramidal and stellate neurons.** (A) Sample trace of a free current-clamp recording from a pyramidal neuron, demonstrating changes in the membrane potential ( $V_m$ ) during normoxia, anoxia and recovery. (B) Sample trace of a free current-clamp recording from a stellate neuron showing changes in  $V_m$  and action potential frequency ( $AP_f$ ). (C) Sample recordings of action potentials by stepwise current injection. (i) In pyramidal neurons, anoxia decreases the probability of action potential generation in response to the same amount of stimulation (1 nA). (ii) In stellate neurons, the probability of action potential firing does not change with anoxia; as a result of  $V_m$  depolarization, firing may increase. (D) Occasionally, an active pyramidal neuron was found ( $n=4$ ); example 1 min traces of spontaneous firing of the active neuron during normoxia and then 5 min of anoxia are shown. (E–G) Summary of changes in:  $V_m$  (E),  $AP_f$  (F) and whole-cell conductance ( $G_w$ ; G) in both pyramidal and stellate neurons for normoxia, anoxia and recovery. With anoxia,  $G_w$  increased in both cell types;  $G_w$  did not change significantly with recovery in either cell type. (H) Changes in  $V_m$  and  $AP_f$  of active pyramidal neurons as in D. Treatments: normoxia: 99%  $O_2$ , 1%  $CO_2$  bubbled artificial cerebrospinal fluid (aCSF); anoxia: 99%  $N_2$ , 1%  $CO_2$  bubbled aCSF; and recovery: 99%  $O_2$ , 1%  $CO_2$  bubbled aCSF. Data are means  $\pm$  s.e.m.,  $n=7$ –14 replicates per treatment and  $n=4$  for active pyramidal neurons. Asterisks indicate a significant difference from baseline normoxia; double daggers indicate a significant difference from normoxic recovery in pyramidal and stellate neural populations:  $*P<0.05$ ,  $**P<0.01$ ,  $***P<0.001$ . n.s., not significant.

quiescent to  $2.23 \pm 0.09$  Hz ( $n=4$ ,  $P<0.001$ ); the increase in  $AP_f$  was not significantly different in stellate neurons ( $AP_f=2.13 \pm 0.02$  Hz,  $n=5$ ) (Fig. 4E). Even though  $AP_f$  drastically increased with GZ+CGP application, in some neurons ( $n=5$ )  $V_m$  hyperpolarized to the pre-anoxia level, neurons became quiescent and stepwise current injection failed to generate an action potential (data not shown). The rest ( $n=4$ ), however, did not recover after GZ+CGP application and continued to generate seizure-like action potentials until loss of  $V_m$ , which is associated with neuronal death (Fig. 4C).

GABA<sub>A/B</sub> receptor antagonism significantly affected  $G_w$  in both pyramidal and stellate neurons. Anoxia increased  $G_w$  from  $3.96 \pm 0.95$  nS to  $6.84 \pm 0.62$  nS ( $P<0.001$ ). Blocking the GABA<sub>A</sub> receptor with GZ had no significant effect on normoxic  $G_w$  ( $2.83 \pm 0.33$  nS,  $P=0.071$ ) but it did significantly block the anoxia-mediated increase ( $3.87 \pm 0.39$  nS,  $P<0.001$ ). Normoxic application of CGP alone did not have an effect on  $G_w$  ( $4.1 \pm 0.56$  nS,  $P=0.81$ ) and application of CGP alone during the anoxic period did not suppress the anoxia-mediated increase ( $5.43 \pm 0.59$  nS,  $P=0.27$ ). Co-application of GZ+CGP did not affect normoxic  $G_w$  ( $3.48 \pm 0.18$  nS,  $P=0.43$ ) but did significantly block the anoxia-mediated increase in  $G_w$  ( $3.7 \pm 0.26$  nS,  $P<0.001$ ). This suggests that the increase in conductance during anoxia is dependent on the activation of GABA<sub>A</sub> receptors and that GABA is likely responsible for anoxic depolarization (Fig. 4F).  $G_w$  measurements were conducted on anoxic and normoxic controls and following treatment with GZ, CGP and GZ+CGP, each with 5 replicates. As the change in  $G_w$  was similar for the two neuronal types, the pharmacological responses were combined. Data are presented as the combined responses of pyramidal and stellate neurons.

## DISCUSSION

In this study we investigated the role of GABAergic neurotransmission in the telencephalon of the naturally anoxia-tolerant goldfish, *C. auratus*. We show that anoxia depolarizes the  $V_m$  of both stellate and pyramidal neurons towards the GABA<sub>A</sub> receptor reversal potential ( $E_{GABA}$ ), which is reversed by application of a GABA<sub>A</sub> receptor blocker. Interestingly, depolarization by increasing GABA<sub>A</sub> receptor currents decreases pyramidal cell  $AP_f$  while it increases the  $AP_f$  of stellate neurons. Furthermore, we show GABA<sub>B</sub>

receptors are also important in anoxic survival as inhibition of both GABA<sub>A</sub> and GABA<sub>B</sub> receptors induce seizure-like activities in telencephalic neurons and apparent cell death. GABA is the primary inhibitory neurotransmitter in the mature mammalian central nervous system and an increase in the extracellular [GABA] seems to be a common response to anoxia in anoxia-tolerant organisms (Krnjevic, 1997; Nilsson and Lutz, 2004; Bickler and Buck, 2007). In the anoxia-tolerant turtle brain (*Chrysemys picta bellii*, *Trachemys scripta elegans*), [GABA] increases by 80-fold, suppressing whole-brain electrical activity by 75–95% (Lutz and Nilsson, 1997). This is strongly mediated by both GABA<sub>A</sub> and GABA<sub>B</sub> receptors, which are critical to anoxic survival of turtle cortical neurons (Pamenter et al., 2011). While turtles become quiescent and enter a stage of minimal activity, goldfish and crucian carp remain slightly active in anoxic waters (Bickler and Buck, 2007). Compared with levels in turtle brain, the anoxia-mediated increase in extracellular [GABA] in crucian carp brain is quite modest and doubles after 5 h of anoxia (Hylland and Nilsson, 1999). Furthermore, with anoxia, GABA removal from the extracellular space is significantly reduced because the expression of GABA transporter proteins decreases by 80%, increasing the effective extracellular [GABA] further (Ellefsen et al., 2009). We observed a significant increase in neuronal  $V_m$  with anoxia. This depolarization led to action potential propagation in stellate neurons while pyramidal neurons remained silent. An increase in AP frequency of stellate neurons seems counter to energy conservation within a low oxygen environment; however, inhibitory neurons consume significantly less energy than excitatory neurons and there are about 10-fold fewer (Howarth et al., 2010). In a study by Hylland and Nilsson (1999), running a high  $[K^+]$  Ringer solution through a microdialysis probe to depolarize the surrounding tissue caused the extracellular [GABA] to increase 14 times, while extracellular [glutamate] doubled. This suggests that the potential for GABA release in crucian carp telencephalon is significantly greater than that for glutamate, resulting in greater GABA release in response to equal amounts of stimulation. If we consider the similarities between the telencephalon of teleost fish and mouse hippocampus, the number of excitatory synapses is approximately 18-fold greater than the number of inhibitory ones (Megías et al., 2001; Muller, 2012). Therefore, as a defense mechanism in goldfish telencephalic neurons, a small population of neurons with high release potential and lower energy requirements are activated to suppress the larger population of excitatory neurons and conserve energy.

In our experiment, blocking NMDA and AMPA receptors failed to suppress action potential firing in stellate neurons while TTX blocked action potentials completely. Therefore, we hypothesized that pathways other than excitatory glutamatergic signaling, such as GABAergic pathways, are responsible for  $V_m$  depolarization during anoxia. Indeed, blocking GABA<sub>A</sub> receptors with GZ reversed anoxic depolarization of  $V_m$  and prevented the anoxia-mediated increase in  $G_w$ . Under physiological conditions, GABA<sub>A</sub> receptors are highly permeable to both  $Cl^-$  and  $HCO_3^-$ ; however, the channels are considerably more permeable to  $Cl^-$  than to  $HCO_3^-$  ( $Cl^-/HCO_3^-$  permeability: 5/1) and, thus, the majority of charge transfer following channel activation is  $Cl^-$  mediated (Errington et al., 2014). Therefore, we conclude that the anoxic increase in  $G_w$  is largely due to the movement of anions.

Measurements of  $E_{GABA}$  revealed that  $V_m$  shifts towards a depolarizing  $E_{GABA}$  with anoxia and induces action potentials in stellate neurons but not in pyramidal cells. This is consistent with a previous report showing exogenous GABA can depolarize goldfish telencephalic gonadotropin-releasing hormone (GnRH) neurons

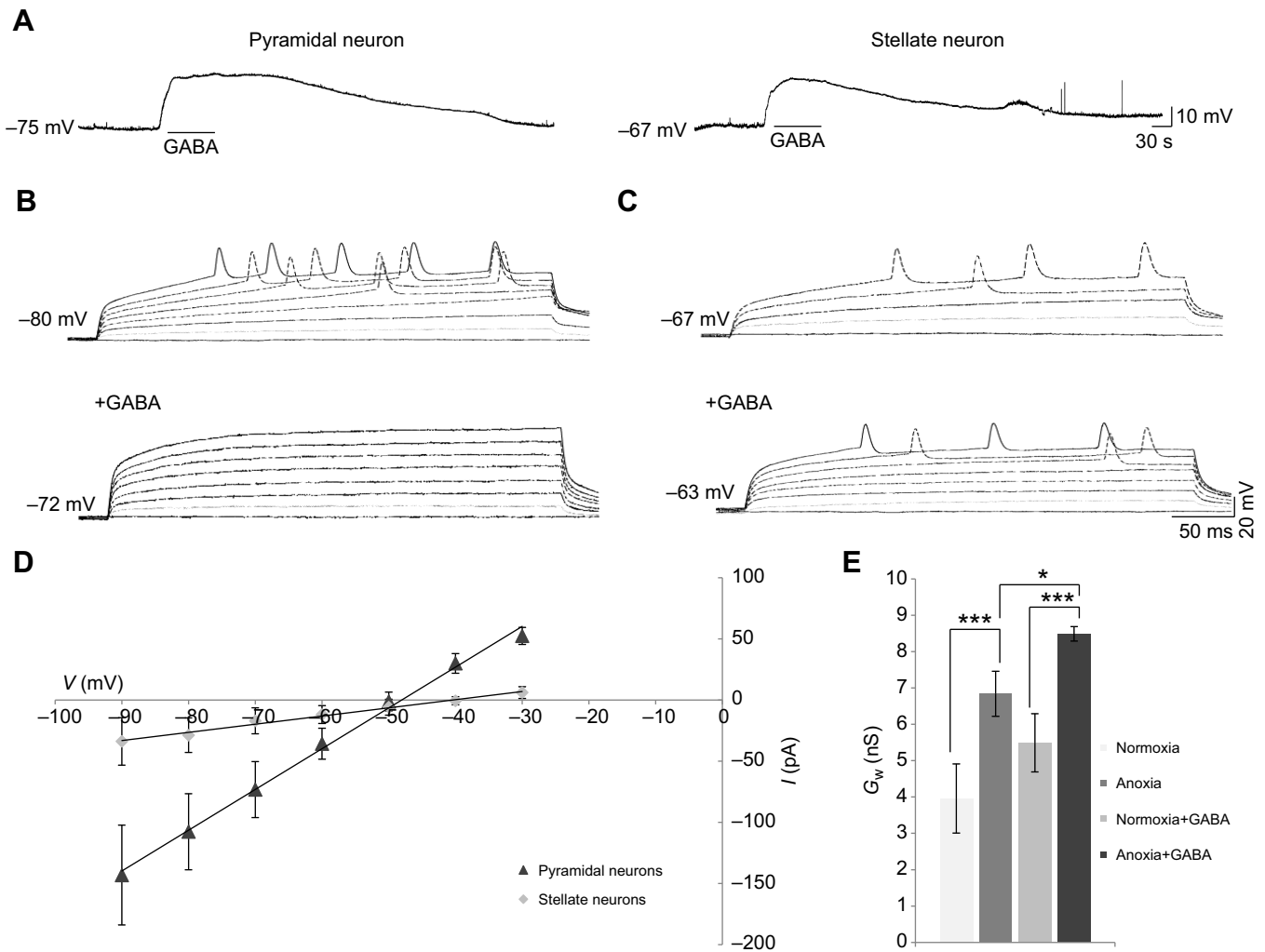


**Fig. 3. Electrophysiological responses of pyramidal and stellate neurons to GABA application.** (A) Passive recordings from pyramidal and stellate neurons during normoxia in the absence and presence of GABA. In both neuronal types, application of GABA increases  $V_m$  during normoxia and  $V_m$  recovers to the initial baseline level minutes after the termination of GABA application. (B,C) Sample recordings of action potentials from pyramidal neurons (B) and stellate neurons (C) following stepwise current injection before and after GABA application during normoxia. (D) Whole-cell current–voltage ( $I/V$ ) relationship from pyramidal and stellate neurons in response to GABA. Application of GABA shifts  $V_m$  towards the GABA reversal potential ( $E_{GABA}$ ). (E) Changes in  $G_w$  in both pyramidal and stellate neurons with and without exogenous GABA application during normoxia and anoxia. Treatments: normoxia: 99%  $O_2$ , 1%  $CO_2$  bubbled aCSF; [GABA], 2 mmol  $l^{-1}$ . Data are means  $\pm$  s.e.m.,  $n=5$ –8 replicates per treatment. Asterisks indicate significance: \* $P < 0.05$ , \*\* $P < 0.01$  and \*\*\* $P < 0.001$ .

(Nakane and Oka, 2010). By changing  $V_m$  to  $E_{GABA}$  in pyramidal neurons, the potential difference between the intracellular and extracellular environments is decreased, which significantly reduces energy in the form of ATP required to maintain ionic gradients (Edwards et al., 1989). Although GABA is depolarizing, it remains inhibitory because it activates an inhibitory shunt that maintains  $V_m$  below the threshold potential (Pamenter et al., 2011).  $E_{GABA}$  is primarily determined by the  $Cl^-$  gradient where  $K^+/Cl^-$ -cotransporter 2 (KCC2) and  $Na^+/K^+/Cl^-$ -cotransporter 1 (NKCC1) set the reversal potential and driving force of anion currents mediated by GABA $_A$  receptors (Blaesse et al., 2009). For GABA to have a depolarizing effect, the intracellular  $[Cl^-]$  must be relatively high (20–25 mmol  $l^{-1}$ ) so that an efflux of  $Cl^-$  occurs via GABA $_A$  receptors (Ben-Ari, 2002). We found that intracellular  $[Cl^-]$  is relatively high in goldfish telencephalic neurons and approximately 1.5 times greater in stellate neurons than in pyramidal neurons. As a result, activation of GABA $_A$  receptors leads to a greater efflux of  $Cl^-$  and further depolarization in stellate neurons compared with pyramidal neurons.  $Cl^-$  flow occurs through both

synaptic (phasic) and extrasynaptic (tonic) GABA receptors (Blaesse et al., 2009). Localization of GABA $_A$  receptors has not been investigated in goldfish neurons; however, crucian carp neurons express the gamma subunit, which is necessary for phasic currents, and delta subunits, which in mammalian brain are extrasynaptic (Mody, 2001; Ellefsen et al., 2009). By applying GZ, we likely inhibited the activity of phasic currents as GZ has a greater affinity for synaptic GABA $_A$  receptors (Mody, 2001). Application of BIC hyperpolarized  $V_m$  of both pyramidal and stellate neurons and reduced  $AP_F$  in stellate neurons similar to GZ. However, BIC blocks both phasic and tonic GABA $_A$  receptors (Ueno et al., 1997), suggesting that the anoxic response is primarily mediated through the activity of the synaptic receptors. Anoxia-tolerant turtle brain differs from goldfish brain as anoxia induces large phasic GABA currents and a 50% increase in tonic current (Hogg et al., 2015). Large phasic GABAergic currents were only observed in a single goldfish pyramidal neuron recordings (1/47 attempts). Perhaps formation of such currents requires an intact circuitry or is localized to a specific cortical region. As our

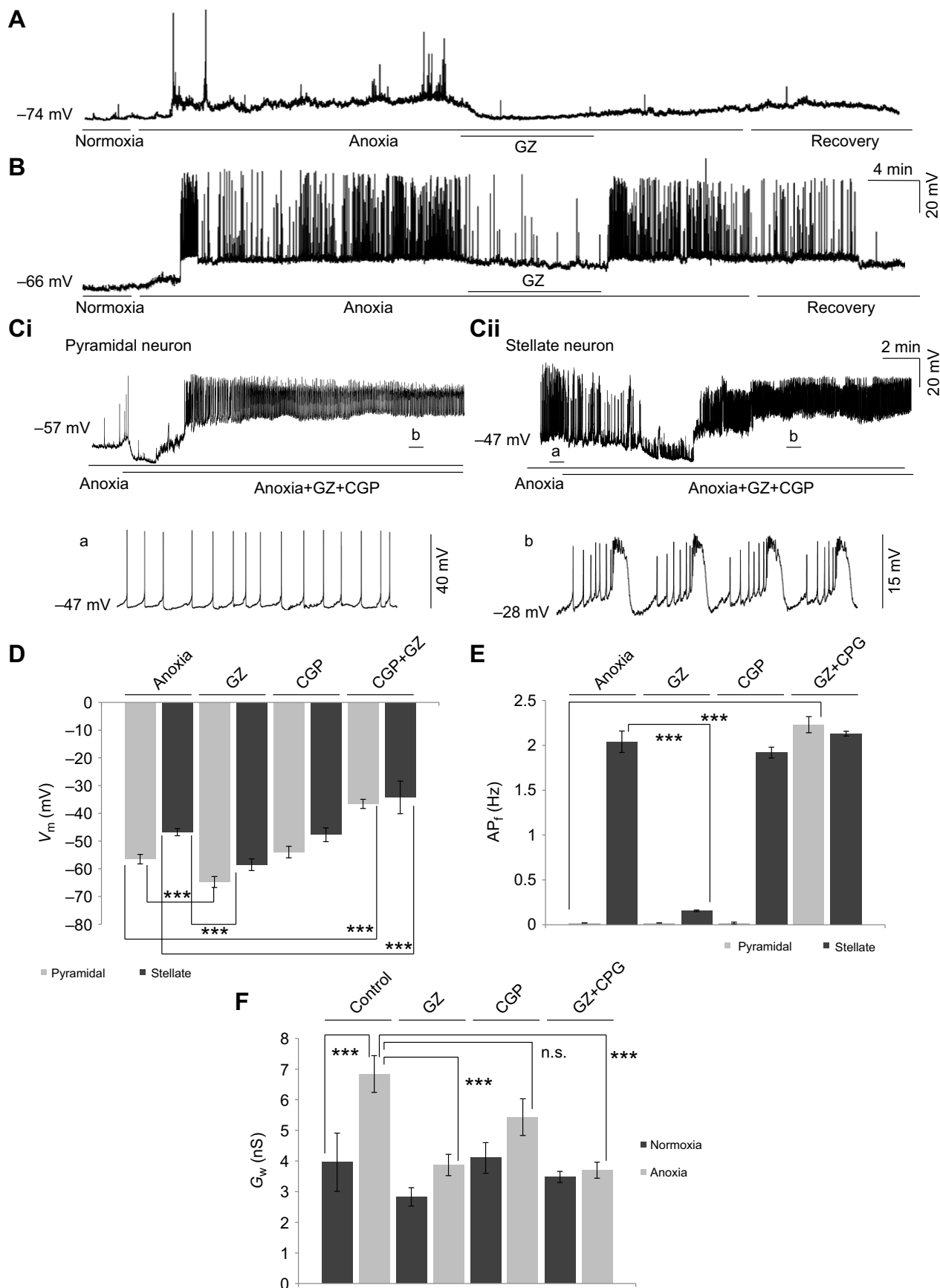


Fig. 4. See next page for legend.



**Fig. 4. Changes in electrophysiological properties in response to GABA receptor inhibition during anoxia.** (A) In pyramidal neurons, application of the GABA<sub>A</sub> receptor inhibitor gabazine (GZ) re-polarized  $V_m$  back to normoxic levels during anoxic exposure. (B) In stellate neurons, similar to pyramidal neurons, GZ re-polarized  $V_m$  and reduced  $AP_f$ .  $V_m$  and  $AP_f$  returned to pre-GZ state with normoxic recovery. (C) Although application of the GABA<sub>B</sub> receptor inhibitor CGP-55845 (CGP) alone did not significantly affect  $V_m$  or  $AP_f$  (data not shown), the combination of GZ+CGP initially hyperpolarized  $V_m$  in both pyramidal (i) and stellate (ii) neurons, similar to that observed with GZ application. With continuous GZ+CGP application,  $V_m$  depolarized in both cell types and led to the generation of sudden seizure-like action potentials. Enlarged traces are shown below; however, only representative traces from stellate neurons are shown because pyramidal neurons were quiescent before drug application and the response was similar after. (D) Changes in  $V_m$  in stellate and pyramidal neurons during anoxia, with application of GZ, CGP and GZ+CGP. GZ hyperpolarized  $V_m$  towards pre-anoxia levels while CGP alone had no significant effect on  $V_m$ . GZ+CGP significantly depolarized  $V_m$ . (E)  $AP_f$  changes with GABA receptor inhibition. GZ had no significant effect on  $AP_f$  in pyramidal neurons; however, it significantly reduced  $AP_f$  in stellate cells. CGP had no significant effect on  $AP_f$  changes in either cell type. GZ+CGP induced seizure-like activities in both neuronal types, significantly increasing the  $AP_f$  in pyramidal cells. (F) Changes in  $G_w$  in both stellate and pyramidal neurons. With anoxia,  $G_w$  increased significantly. GZ and GZ+CGP significantly reduced the anoxic  $G_w$  while CGP alone had no significant effect on anoxic conductance. No significant change was observed following drug application during normoxia ( $G_w$  data were recorded immediately after drug application). Treatments: normoxia: 99% O<sub>2</sub>, 1% CO<sub>2</sub> bubbled aCSF; anoxia: 99% N<sub>2</sub>, 1% CO<sub>2</sub> bubbled aCSF. [GZ], 25  $\mu\text{mol l}^{-1}$ , [CGP], 5  $\mu\text{mol l}^{-1}$ .  $n=5-9$  for each treatment. Asterisks indicate significance: \* $P<0.05$ , \*\* $P<0.01$  and \*\*\* $P<0.001$ . n.s., not significant.

electrophysiological recordings were from brain slices, the circuitry might have been disrupted (Dukoff et al., 2014; Hogg et al., 2015). Furthermore, all the recordings utilized the blind-patch technique, which prevents clear localization of the areas populated with neurons that induce large GABA-mediated currents (Blanton et al., 1989). As a result of such limitations and the inability to frequently record GABA-induced currents, it is not possible to state to what degree tonic GABA<sub>A</sub> receptors are involved in the anoxic response in the goldfish brain.

Blocking GABA<sub>B</sub> receptors alone did not affect  $V_m$  or  $AP_f$  and changes in  $G_w$  were not as strong as those during GABA<sub>A</sub> receptor inhibition. These receptors are slow acting (100–500 ms) G-protein coupled inwardly rectifying potassium channels (GIRKs) and mediate prolonged neural inhibition by increasing K<sup>+</sup> efflux via K<sup>+</sup> channels post-synaptically and inhibiting voltage-gated Ca<sup>2+</sup> channels pre-synaptically (Gassmann and Bettler, 2012). GABA<sub>B</sub> receptor activity is strongly mediated by intracellular messenger mechanisms (Kuramoto et al., 2007). With anoxia or a shortage of ATP, certain intracellular signaling proteins, such as AMP-dependent protein kinase (AMPK), are activated due to an increase in [AMP] (Carling, 2004). AMP has a critical role in maintaining cellular and systemic energy balance and promoting glycolysis (Stensl  kken et al., 2008). Through phosphorylation, AMPK strongly enhances GABA<sub>B</sub> receptor activity, allowing a greater K<sup>+</sup> efflux via GIRKs (Kuramoto et al., 2007). Anoxic exposure significantly increases AMPK phosphorylation in crucian carp brain (Stensl  kken et al., 2008).

In this study, we were able to show that inhibition of both GABA<sub>A</sub> and GABA<sub>B</sub> receptors leads to sudden, uncontrollable electrical activity and a paroxysmal depolarizing shift. The paroxysmal depolarizing shift is a manifestation of neural epilepsy that is in contrast to endogenous burst firing as it is network driven (Johnston and Brown, 1984). In some neurons,  $V_m$  did not return to baseline and seizure-like activities persisted. In others,  $V_m$  hyperpolarized to a pre-anoxic stage after hyperactivity

and cells became quiescent. This does not necessarily imply that these neurons recovered from seizure as this can occur as a result of a depolarization block in which seizure can be maintained even in the absence of continuous neuronal firing (Bikson et al., 2003). While co-antagonism of GABA<sub>A</sub> and GABA<sub>B</sub> receptors induced paroxysmal depolarizing shift, blocking either GABA<sub>A</sub> or GABA<sub>B</sub> receptors alone did not cause catastrophic depolarization. GABA<sub>A</sub> and GABA<sub>B</sub> receptors have a complementary role in reducing neural excitation (Mann et al., 2009). GZ significantly reduced conductance and reversed the anoxic depolarization; however, GABA<sub>B</sub> receptors might prevent the release of excitatory neurotransmitters and excitotoxic cell death even when GABA<sub>A</sub> receptors are inactive. In the anoxic turtle brain, GABA<sub>B</sub> receptors predominantly act pre-synaptically and decrease excitatory post-synaptic potentials (EPSPs), especially AMPAergic EPSPs (Pamenter et al., 2011). Furthermore, we show that inhibiting GABA<sub>B</sub> receptors alone does not significantly change the anoxic  $G_w$  while blocking GABA<sub>A</sub> receptors does. This suggests that the major change in conductance brought on by anoxia must occur through GABA<sub>A</sub> receptors and could explain why application of CGP alone causes no catastrophic depolarization. Activity of GABA<sub>B</sub> receptors may be crucial to neural survival and limiting excitotoxicity, especially if GABA<sub>A</sub> receptors are inactive, perhaps by decreasing EPSPs and reducing neurotransmitter release (Kuramoto et al., 2007; Pamenter et al., 2011; Tao et al., 2013).

In conclusion, we report that in anoxic goldfish telencephalic stellate neurons,  $AP_f$  increases while pyramidal neuron  $AP_f$  or the potential to generate action potentials is decreased. In both neuronal types,  $V_m$  depolarizes towards the  $E_{\text{GABA}}$  but because  $E_{\text{GABA}}$  is more depolarizing in stellate neurons, it is responsible for the increased activity. Inhibiting both GABA<sub>A</sub> and GABA<sub>B</sub> receptors induces terminal depolarization of goldfish neurons, highlighting the importance of GABA in anoxia tolerance.

#### Acknowledgements

The authors would like to thank Dr Kaori Takehara-Nishiuchi and Dr Martin Wojtowicz for their valuable insights and critiques during every stage of this study.

#### Competing interests

The authors declare no competing or financial interests.

#### Author contributions

Conceptualization: L.T.B., N.H.-J.; Methodology: N.H.-J., W.E.L.; Formal analysis and investigation: N.H.-J., W.E.L., L.T.B.; Writing - original draft preparation: N.H.-J.; Writing - review and editing: L.T.B., N.H.-J.; Funding acquisition: L.T.B., M.P.W.; Resources: L.T.B.; Supervision: L.T.B.

#### Funding

This study was supported by the Natural Sciences and Engineering Research Council (NSERC Discovery Grant) to L.T.B. (06588) and M.P.W. (04248).

#### References

- Ben-Ari, Y. (2002). Excitatory actions of GABA during development: the nature of the nurture. *Nat. Rev. Neurosci.* **3**, 728–739.
- Bickler, P. E. and Buck, L. T. (2007). Hypoxia tolerance in reptiles, amphibians and fishes: life with variable oxygen availability. *Annu. Rev. Physiol.* **69**, 145–170.
- Bikson, M., Hahn, P. J., Fox, J. E. and Jefferys, J. G. R. (2003). Depolarization block of neurons during maintenance of electrographic seizures. *J. Neurophysiol.* **90**, 2402–2408.
- Blaesse, P., Airaksinen, M. S., Rivera, C. and Kaila, K. (2009). Cation-chloride cotransporters and neuronal function. *Neuron* **61**, 820–838.
- Blanton, M. G., Lo Turco, J. J. and Kriegstein, A. R. (1989). Whole cell recording from neurons in slices of reptilian and mammalian cerebral cortex. *J. Neurosci. Methods* **30**, 203–210.
- Buck, L. T. and Hochachka, P. W. (1993). Anoxic suppression of Na(+)-K(+)-ATPase and constant membrane potential in hepatocytes: support for channel arrest. *Am. J. Physiol.* **265**, 1020–1025.

- Carling, D. (2004). The AMP-activated protein kinase cascade—a unifying system for energy control. *Trends Biochem. Sci.* **29**, 18–24.
- Connors, B. W. and Kriegstein, A. R. (1986). Cellular physiology of the turtle visual cortex: distinctive properties of pyramidal and stellate neurons. *J. Neurosci.* **6**, 164–177.
- Dukoff, D. J., Hogg, D. W., Hawrysh, P. J. and Buck, L. T. (2014). Scavenging ROS dramatically increases NMDA receptor whole cell currents in painted turtle cortical neurons. *J. Exp. Biol.* **217**, 3346–3355.
- Edwards, R. A., Lutz, P. L. and Baden, D. G. (1989). Relationship between energy expenditure and ion channel density in the turtle and rat brain. *Am. J. Physiol.* **257**, 1354–1358.
- Ellefsen, S., Stenslokken, K.-O., Fagernes, C. E., Kristensen, T. A. and Nilsson, G. E. (2009). Expression of genes involved in GABAergic neurotransmission in anoxic crucian carp brain (*Carassius carassius*). *Physiol. Genomics* **36**, 61–68.
- Erecińska, M. and Silver, I. A. (1994). Ions and energy in mammalian brain. *Prog. Neurobiol.* **43**, 37–71.
- Errington, A. C., Di Giovanni, G. and Crunelli, V. (2014). *Extrasynaptic GABA<sub>A</sub> Receptors*. Heidelberg: Springer.
- Gassmann, M. and Bettler, B. (2012). Regulation of neuronal GABA<sub>B</sub> receptor functions by subunit composition. *Nat. Rev. Neurosci.* **13**, 380–394.
- Hansen, A. J. (1985). Effect of anoxia on ion distribution in the brain. *Physiol. Rev.* **65**, 101–148.
- Hochachka, P. W. (1986). Defense strategies against hypoxia and hypothermia. *Science* **231**, 234–241.
- Hochachka, P. W., Buck, L. T., Doll, C. J. and Land, S. C. (1996). Unifying theory of hypoxia tolerance: molecular/metabolic defense and rescue mechanisms for surviving oxygen lack. *Proc. Natl. Acad. Sci.* **93**, 9493–9498.
- Hogg, D. W., Pamenter, M. E., Dukoff, D. J. and Buck, L. T. (2015). Decreases in mitochondrial reactive oxygen species initiate GABA<sub>A</sub> receptor-mediated electrical suppression in anoxia-tolerant turtle neurons. *J. Physiol.* **593**, 2311–2326.
- Howarth, C., Peppiatt-Wildman, C. M. and Attwell, D. (2010). The energy use associated with neural computation in the cerebellum. *J. Cereb. Blood Flow Metab.* **30**, 403–414.
- Hylland, P. and Nilsson, G. E. (1999). Extracellular levels of amino acid neurotransmitters during anoxia and forced energy deficiency in crucian carp brain. *Brain Res.* **823**, 49–58.
- Johnston, D. and Brown, T. H. (1984). The synaptic nature of the paroxysmal depolarizing shift in hippocampal neurons. *Ann. Neurol.* **16**, S65–S71.
- Krnjevic, K. (1997). Role of GABA in cerebral cortex. *Can. J. Physiol. Pharmacol.* **75**, 439–451.
- Kuramoto, N., Wilkins, M. E., Fairfax, B. P., Revilla-sanchez, R., Terunuma, M., Tamaki, K., Lemata, M., Warren, N., Couve, A., Calver, A., (2007). Phospho-dependent functional modulation of GABA(B) receptors by the metabolic sensor AMP-dependent protein kinase. *Neuron* **53**, 233–247.
- Larkum, M. E., Watanabe, S., Lasser-Ross, N., Rhodes, P. and Ross, W. N. (2008). Dendritic properties of turtle pyramidal neurons. *J. Neurophysiol.* **99**, 683–694.
- Lutz, P. L. (1992). Mechanisms for anoxic survival in the vertebrate brain. *Annu. Rev. Physiol.* **54**, 601–618.
- Lutz, P. L. and Nilsson, G. E. (1997). Contrasting strategies for anoxic brain survival—glycolysis up or down. *J. Exp. Biol.* **200**, 411–419.
- Mann, E. O., Kohl, M. M. and Paulsen, O. (2009). Distinct role of GABA<sub>A</sub> and GABA<sub>B</sub> receptors in balancing and terminating persistent cortical activity. *J. Neurosci.* **29**, 7513–7518.
- Megías, M., Emri, Z., Freund, T. F. and Gulyás, A. L. (2001). Total number and distribution of inhibitory and excitatory synapses on hippocampal CA1 pyramidal cells. *Neuroscience* **102**, 527–540.
- Melendez-Ferro, M., Prez-Costas, E. and Roberts, R. C. (2009). A new use for long-term frozen brain tissue: golgi impregnation. *J. Neurosci. Methods* **176**, 72–77.
- Mody, I. (2001). Distinguishing between GABA(A) receptors responsible for tonic and phasic conductances. *Neurochem. Res.* **26**, 907–913.
- Muller, T. (2012). What is the thalamus in zebrafish? *Front. Neurosci.* **6**, 64.
- Nakane, R. and Oka, Y. (2010). Excitatory action of GABA in the terminal nerve gonadotropin-releasing hormone neurons. *J. Neurophysiol.* **103**, 1375–1384.
- Nilsson, G. E. and Lutz, P. (2004). Anoxia tolerant brains. *J. Cereb. Blood Flow Metab.* **24**, 475–486.
- Olude, M. A., Mustapha, O. A., Aderounmu, O. A., Olopade, J. O. and Ihunw, A. O. (2015). Astrocyte morphology, heterogeneity, and density in the developing African giant rat (*Cricetomys gambianus*). *Front. Neuroanat.* **9**, 1–10.
- Pamenter, M. E., Hogg, D. W., Ormond, J., Shin, D. S., Woodin, M. A. and Buck, L. T. (2011). Endogenous GABA<sub>A</sub> and GABA<sub>B</sub> receptor-mediated electrical suppression is critical to neuronal anoxia tolerance. *Proc. Natl. Acad. Sci.* **108**, 11274–11279.
- Peter, R. E. and Gill, V. E. (1975). A stereotaxic atlas and technique for forebrain nuclei of the goldfish, *Carassius auratus*. *J. Comp. Neurol.* **159**, 69–101.
- Sattler, R. and Tymianski, M. (2000). Molecular mechanisms of calcium-dependent excitotoxicity. *J. Mol. Med.* **78**, 3–13.
- Shepherd, G. M. (2011). The microcircuit concept applied to cortical evolution: from three-layer to six-layer cortex. *Front. Neuroanat.*
- Shin, D. S. and Buck, L. T. (2003). Effect of anoxia and pharmacological anoxia on whole-cell NMDA receptor currents in cortical neurons from the western painted turtle. *Physiol. Biochem. Zool.* **76**, 41–51.
- Stenslokken, K.-O., Ellefsen, S., Stecyk, J. A. W., Dahl, M. B., Nilsson, G. E. and Vaage, J. (2008). Differential regulation of AMP-activated kinase and AKT kinase in response to oxygen availability in crucian carp (*Carassius carassius*). *Am. J. Physiol. Regul. Integr. Comp. Physiol.* **295**, 1803–1814.
- Tao, W., Higgs, M. H., Spain, W. J. and Ransom, C. B. (2013). Postsynaptic GABAB receptors enhance extrasynaptic GABAA receptor function in dentate gyrus granule cells. *J. Neurosci.* **33**, 3738–3743.
- Ueno, S., Bracamontes, J., Zorumski, C., Weiss, D. S. and Steinbach, J. H. (1997). Bicuculline and gabazine are allosteric inhibitors of channel opening of the GABAA receptor. *J. Neurosci.* **17**, 625–634.
- Watanabe, M., Wake, H., Moorhouse, A. J. and Nabekura, J. (2009). Clustering of neuronal K<sup>+</sup>-Cl<sup>-</sup> cotransporters in lipid rafts by tyrosine phosphorylation. *J. Biol. Chem.* **284**, 27980–27988.
- Wilkie, M. P., Pamenter, M. E., Alkabie, S., Carapic, D., Shin, D. S. and Buck, L. T. (2008). Evidence of anoxia-induced channel arrest in the brain of the goldfish (*Carassius auratus*). *Comp. Biochem. Physiol. C. Toxicol. Pharmacol.* **148**, 355–362.